Effects of Magnetic Fields on Microbiologically Influenced Corrosion of 304 Stainless Steel

ARTICLE *in* INDUSTRIAL & ENGINEERING CHEMISTRY RESEARCH · DECEMBER 2013

Impact Factor: 2.59 · DOI: 10.1021/ie402235j

4 AUTHORS, INCLUDING:

H. Liu
Huazhong University of Science and Technology
78 PUBLICATIONS **464** CITATIONS

SEE PROFILE

I&EC research
Industrial & Engineering Chemistry Research

Article

pubs.acs.org/IECR

Effects of Magnetic Fields on Microbiologically Influenced Corrosion of 304 Stainless Steel

Bijuan Zheng,[†,§] Kejuan Li,[†,§] Hongfang Liu,[†,*] and Tingyue Gu[‡]

[†]School of Chemistry and Chemical Engineering, Hubei Key Laboratory of Materials Chemistry and Service Failure, Huazhong University of Science and Technology, Wuhan 430074, China

[‡]Department of Chemical and Biomolecular Engineering, Institute for Corrosion and Multiphase Technology, Ohio University, Athens Ohio 45701, United States

ABSTRACT: The effects of magnetic fields (MFs) on the corrosion of 304 stainless steel (SS304) caused by oil-field sulfate-reducing bacteria (SRB) were investigated. Experimental data showed that the MF lowered the population of planktonic SRB by almost 4 orders of magnitude and delayed the formation of SRB biofilms on the SS304 coupons. The mass losses and surface images of the coupons indicated that the application of an MF considerably reduced the pitting corrosion of SS304. EDX and XPS analyses of the coupon surfaces demonstrated that the main corrosion products without an MF and with 2 and 4 mT MFs were FeS, FeO, and Fe_2O_3, respectively. The application of MFs could be an environmentally friendly method for mitigating microbiologically influenced corrosion (MIC) on SS304.

1. INTRODUCTION

The effects of magnetic fields (MFs) in metal corrosion have been extensively studied in recent years. Much research has focused on the effects of MFs on the abiotic electrochemical corrosion of stainless steel,[1] iron,[2,3] and cooper[4,5] in sulfuric acid and in weakly alkaline and neutral solutions.[6−9] The effects of MFs on metal corrosion can be explained in terms of the field-assisted development of a passivation layer,[1] the Lorentz force, and the MF gradient force,[2,3] as well as the impact on the surface pH value.[10] Corrosion rates of stainless steel and copper have been found to be significantly reduced in the presence of a magnetic field.[1,4] However, the application of an MF was found to accelerate the corrosion of a Nd−Fe−B magnet in a naturally aerated 3.5 wt % NaCl solution,[11] where the difference in the specimens' corrosion rates was ascribed to enhanced transport of oxygen in the bulk solution to the magnet/electrolyte interface as a result of the presence of MF.

MFs can also influence living organisms. Many studies have shown that the amount of bacteria and their viability decrease at longer exposure times, higher temperatures and higher magnetic field intensities,[12−14] but the quantity of the effect is species-dependent.[13] The mechanism has been explored in terms of parameters such as cell wall integrity,[13] enzymatic activity and ATP level,[15] cytoskeleton,[16] and glutathione (GSH) and biomass concentrations.[17]

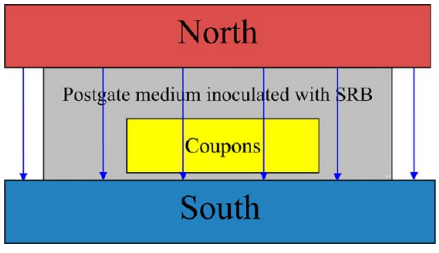

Figure 1. Experimental setup of the magnetic field.

Sulfate-reducing bacteria (SRB), which reduce sulfate to sulfide in their metabolism, are one of the most common types of microbes associated with microbiological influenced corrosion (MIC).[18−22] Sessile SRB cells in a biofilm on a metal surface are capable of transferring extracellular electrons from the oxidation of elemental iron (Fe^0) into their cytoplasm, where sulfate reduction occurs under enzyme catalysis. Because planktonic cells cannot transfer the extracellular electrons across a body of aqueous solution, they are not directly involved in this type of MIC. MIC of steel is a serious problem in the marine

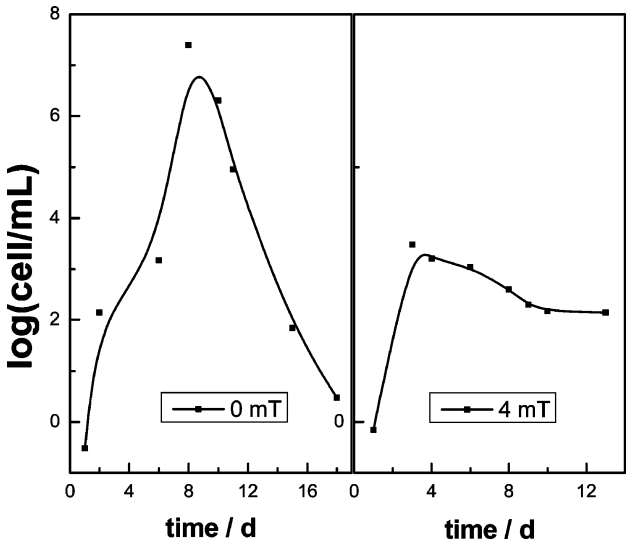

Figure 2. Growth curve of planktonic SRB without a magnetic field and under a 4 mT magnetic field.

Received: July 13, 2013
Revised: November 12, 2013
Accepted: December 7, 2013
Published: December 8, 2013

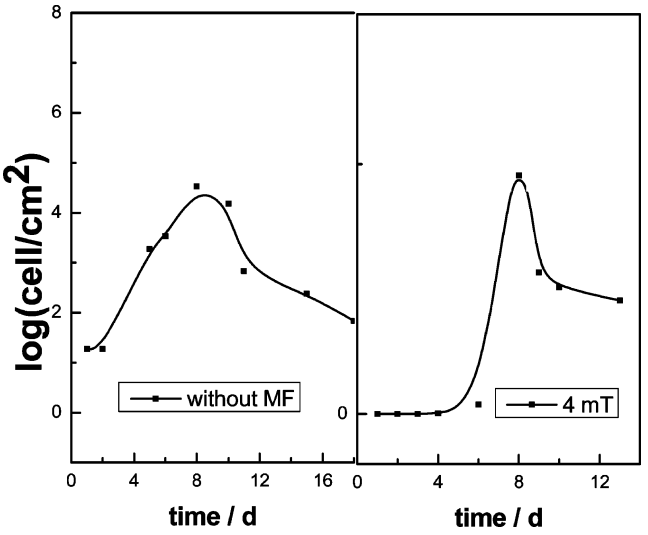

Figure 3. Growth curve of a sessile SRB population without a magnetic field and under a 4 mT magnetic field.

environment and many industries, such as oil and gas, power generation, and paper manufacturing, with serious safety and economic concerns.[23,24] As already mentioned, MFs can influence not only the growth of microorganisms but also the electrochemical process, mass transfer, and corrosion products.

Table 1. Corrosion Mass Loss of SS304 after 14-Day Exposure to SRB Culture with and without a Magnetic Field

magnetic field (mT)	mass loss ($mg \cdot cm^{-2}$)	average corrosion rate ($mm \cdot y^{-1}$)
0	7.9 ± 2.7	0.1504
2	2.6 ± 1.2	0.0457
4	1.9 ± 0.3	0.0328

The present research was aimed at exploring the effects of MFs on the MIC of 304 stainless steel (SS304) caused by SRB in terms of SRB growth, corrosion extent, and corrosion products.

2. EXPERIMENTAL MATERIALS AND METHODS

The nominal composition of the SS304 coupons used in this study was 8.0−11.0% Ni, 17.0−19.0% Cr, ≤2.0% Mn, ≤1.0% Si, ≤0.03% S, ≤0.035% P, ≤0.07% C, and the balance Fe. Disk-shaped SS304 coupons with a diameter of 15 mm and a thickness of 2 mm were used throughout this work. SRB were isolated from an oil field and enriched in Postgate culture medium.[25] The culture medium contained (per liter of distilled water) 4.0 mL of sodium lactate 60% (w/w) syrup, 1.0 g of yeast extract, 0.1 g of vitamin C, 0.2 g of $MgSO_4 \cdot 7H_2O$, 0.01 g of K_2HPO_4, and 10.0 g of NaCl. The pH was adjusted to 7.0−7.2 using 1 mol/L NaOH. The medium was sterilized in an autoclave at 1.2×10^4 Pa for 20 min. After the medium had been allowed to cool to room temperature, 0.2 g of $(NH_4)_2SO_4 \cdot 6H_2O$

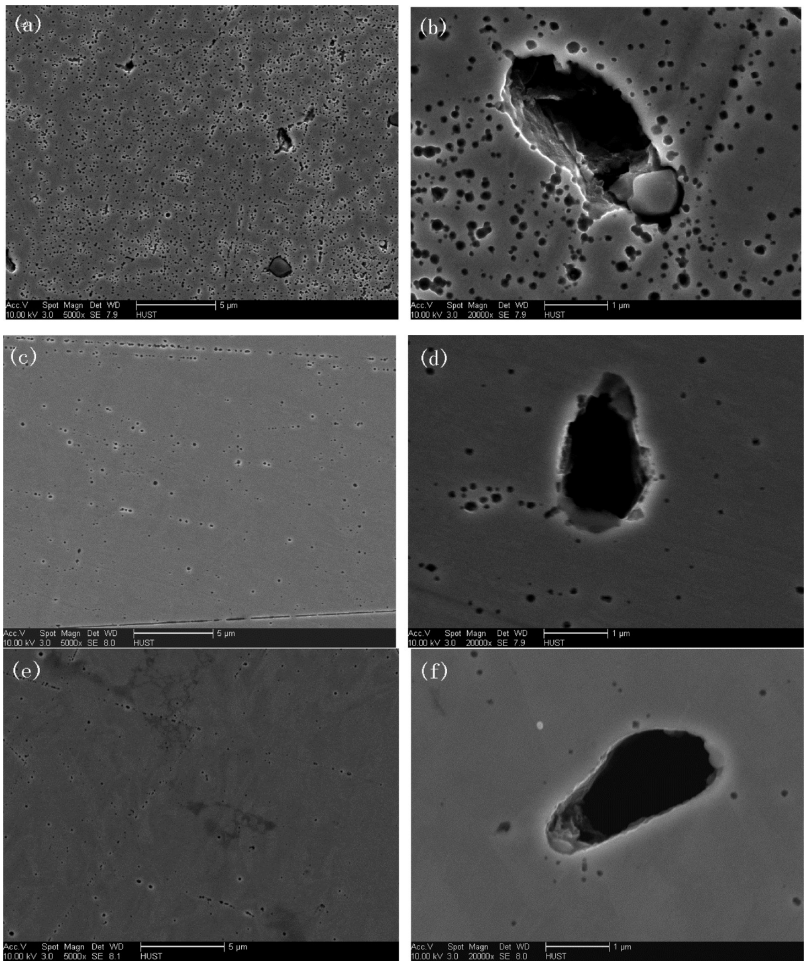

Figure 4. SEM images of SS304 free of biofilms and corrosion products after 14-day exposure in SRB culture (a,b) without a magnetic field, (c,d) with a 2 mT magnetic field, and (e,f) with a 4 mT magnetic field.

dx.doi.org/10.1021/ie402235j | Ind. Eng. Chem. Res. 2014, 53, 48−54

Table 2. Number of Pits and Sizes of Representative Pits on SS304 Coupons after 14-Day Exposure to SRB Culture

		representative pit size		
magnetic field (mT)	number of the pits per unit area (μm^{-2})	length (μm)	width (μm)	depth (μm)
0	120 ± 30	3.4	1.6	2.0
2	18 ± 3	2.2	1.2	0.4
4	9 ± 1	2.8	1.2	0.8

that had been sterilized with ultraviolet light was added to each liter of the culture medium. The experimental setup is shown in Figure 1. The bioreactor contained 120 mL of culture medium. A 10 mL planktonic SRB seed culture was used to inoculate the sterilized culture medium to grow planktonic and sessile SRB cells. For sessile SRB growth, three SS304 coupons were placed separately on the bottom of the bioreactor as the substratum. For comparison, coupons exposed to the SRB culture without any MF served as controls. After 2 weeks of incubation at 37 °C, coupons were withdrawn for analysis. The SRB biofilm on each coupon was scraped off and suspended in 5 mL of sterile medium. The SRB cell count (cells/mL) in the medium was obtained using the most probable number (MPN) method,[26] and the cell count was then converted to the sessile cell count (cells/cm^2) based on the coupon surface area covered by the biofilm. The corrosion rate was measured by the mass loss method. The average from three duplicate coupons was used to obtain each mass loss data point.

Microscope images of the biofilms and corrosion products on the coupon surfaces were obtained using a Sirion 200 field-emission scanning electron microscope (FEI, Eindhoven, The Netherlands) equipped with energy-dispersive X-ray (EDX) detectors for elemental analysis. Sulfur, iron, and oxygen valence states were determined by X-ray photoelectron spectroscopy (XPS) with a Multilab 2000 spectrometer (VG Instruments Group Ltd., Guildford, Surrey, U.K.) equipped with a monochromatic Mg Kα X-ray source. The operating current and potential of the X-ray generator were 16 mA and 12.5 kV, respectively. The residual pressure inside the analytical chamber was less than 2×10^{-9} Pa.

3. RESULTS AND DISCUSSION

3.1. Growth Curves of Planktonic SRB and Sessile SRB.

The growth curves of planktonic SRB and sessile SRB biofilm without an MF and under a 4 mT MF are shown in Figures 2 and 3. The maximum planktonic SRB population in the control was 2.5×10^7 cell/mL on the eighth day, whereas the maximum planktonic SRB population under the MF was 3×10^3 cell/mL

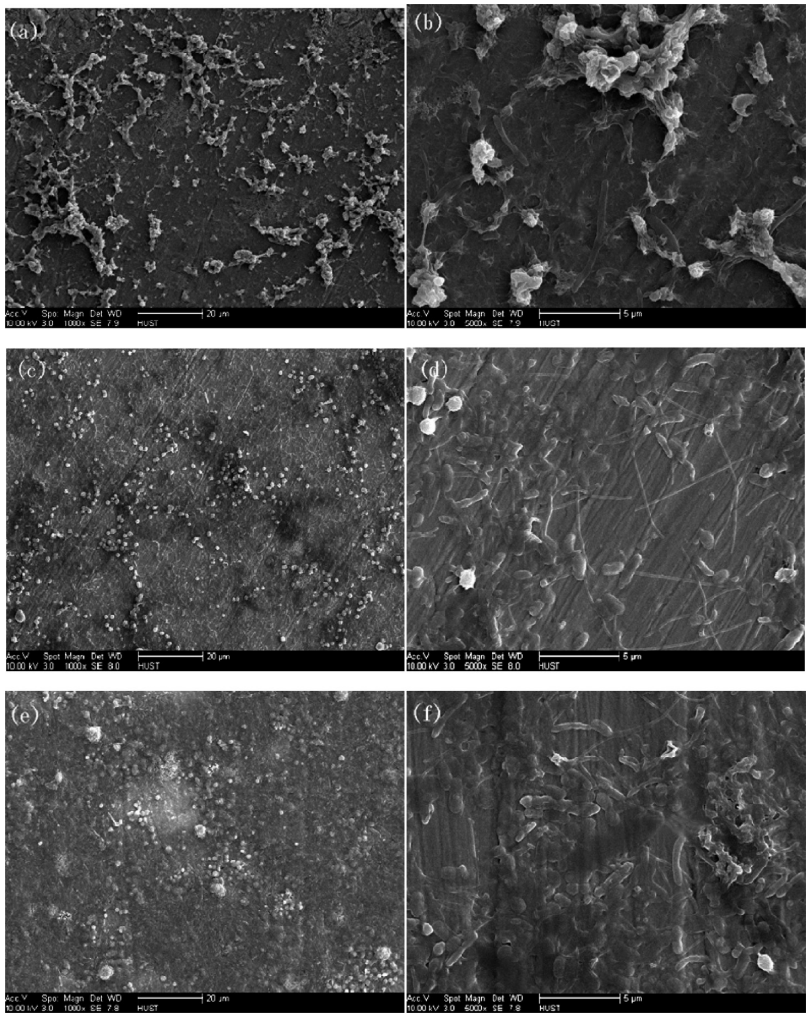

Figure 5. SEM images of SRB biofilms on SS304 after 14-day exposure in SRB culture (a,b) without a magnetic field, (c,d) with a 2 mT magnetic field, and (e,f) with a 4 mT magnetic field.

dx.doi.org/10.1021/ie402235j | Ind. Eng. Chem. Res. 2014, 53, 48−54

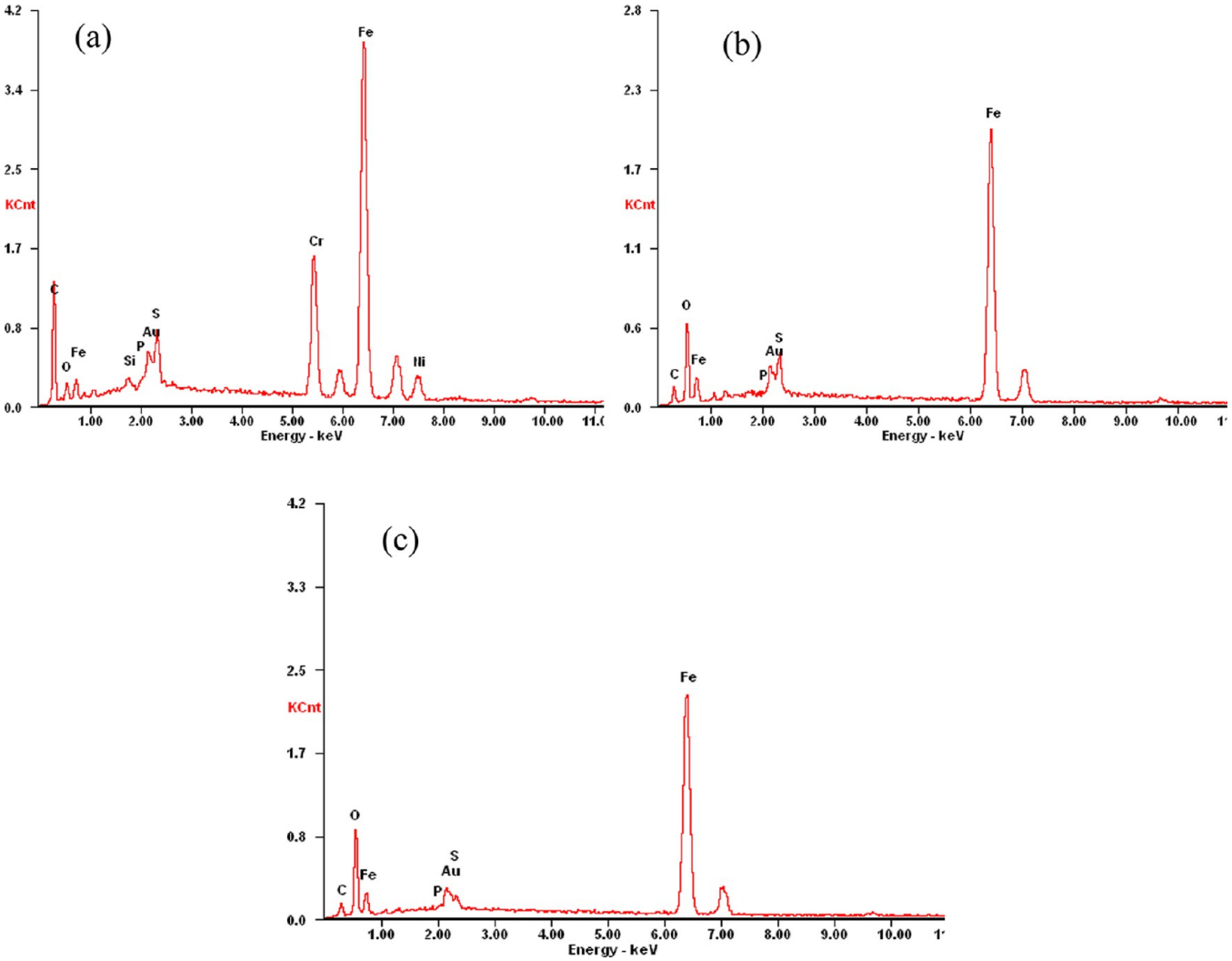

Figure 6. Energy-dispersive X-ray (EDX) analysis of corrosion products on the surface of SS304 after 14-day exposure in SRB culture (a) without a magnetic field, (b) with a 2 mT magnetic field, and (c) with a 4 mT magnetic field.

on the third day. This suggests that the MF reduced the population of planktonic SRB by almost 4 orders of magnitude.

In MIC, pitting can be initiated underneath biofilms. Sessile cells, rather than planktonic cells, are directly responsible for MIC. In Figure 3, the maximum sessile SRB populations with a 4 mT MF and without an MF (control) were both about 10^4 cell/cm^2 on the eighth day. However, the 4 mT MF delayed the takeoff of the sessile cell count by at least two days.

3.2. Corrosion Rate. The corrosion mass losses of SS304 coupons immersed in SRB cultures for 14 days are listed in Table 1. Compared with the control without an MF, the mass losses of SS304 coupons in the SRB cultures decreased by 67.1% and 76.4% under 2 and 4 mT MFs, respectively.

The extent of pitting corrosion damage caused by the SRB was assessed by profiling the pits on the coupon surface after removal of the biofilms and corrosion products. As shown in Figure 4, the SRB caused serious pitting corrosion to SS304. The numbers of the pits per unit area and the sizes of representative pits are listed in Table 2. Table 2 shows that application of an MF not only greatly reduced the numbers of pits on the coupon surfaces but also significantly shrank the sizes of representative pits. These images also demonstrate that the 4 mT MF more effectively inhibited SRB pitting corrosion than the 2 mT MF. This finding is in good agreement with the results for corrosion mass loss. In this work, only two MF intensities were used. A future study to find the optimized intensity is desired.

3.3. Corrosion Products. Figure 5 shows SEM images of the SS304 coupon surfaces after 14-day exposure to SRB without an MF and with 2 and 4 mT MFs to show the differences in the biofilms. Figure 5a,b demonstrates that, in a natural environment (i.e., no MF), SRB biofilms tended to create heterogeneous surface conditions. This spatial structure of the biofilms has very important effects on metal corrosion.[27] Thin biofilms formed on the SS304 coupon surfaces in the presence of the MFs, as shown in Figure 5d,f. Compared with Figure 5a (without an MF), there were obviously fewer SRB colonies on the coupons for both the 2 mT MF (Figure 5c) and the 4 mT MF (Figure 5e).

The elements of C, O, Si, P, S, Fe, Cr, Au, and Ni were all detected on the control coupon, as shown in Figure 6a. Au was introduced during coupon preparation for SEM through sputtering to make the biofilm surface conductive. In contrast to the control coupon, another significant feature for the two coupons exposed to MFs was the abundance of the O signal and the weakness of the S signal in the surface film (Figure 6b,c), whereas much less O was detected on the control coupon.

dx.doi.org/10.1021/ie402235j | Ind. Eng. Chem. Res. 2014, 53, 48−54

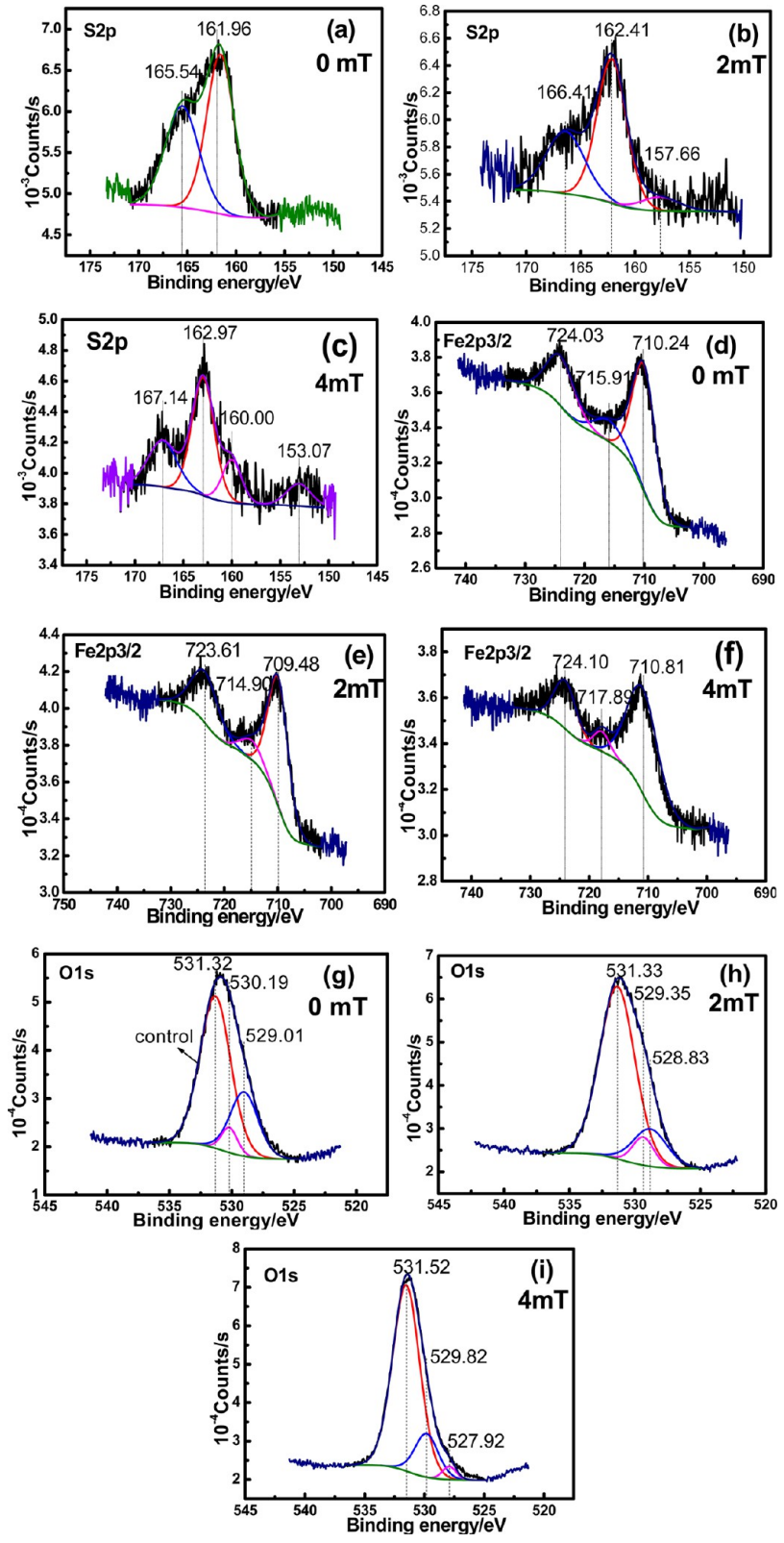

Figure 7. (a–c) S 2p, (d–f) Fe $2p_{3/2}$, and (g–i) O 1s XPS spectra of corrosion products on SS304 after 14-day exposure in SRB culture: (a,d,g) without a magnetic field, (b,e,h) with a 2 mT magnetic field, and (c,f,i) with a 4 mT magnetic field.

To better understand the differences in the chemical compositions of the corrosion products on SS304, XPS was employed to acquire the S 2p, Fe 2p, and O 1s spectra of the 14-day coupon surfaces, as shown in Figure 7. The binding energies and the corresponding species are listed in Table 3. The distinctive peak components of the three types of Fe $2p_{3/2}$ spectra are attributed to FeS (specific binding energy = 710.3 eV), FeO (specific binding energy = 709.4 eV), and Fe_2O_3 (specific binding energy = 710.8 eV).[28] Fe existed as FeS on the control coupon, while the S 2p spectrum at binding energy of 161.96 eV obtained

dx.doi.org/10.1021/ie402235j | Ind. Eng. Chem. Res. 2014, 53, 48–54

Table 3. Electronic Binding Energies Corresponding to S- and Fe-Containing Species

magnetic field (mT)	E(S 2p) (eV)	species	E(Fe $2p_{3/2}$) (eV)	species
0	161.96, 165.54	Fe**S**, Na_2SO_3	710.24	**Fe**S
2	162.13, 166.41	Na_2SSO_3, Na_2SO_3	709.48	**Fe**O
4	162.97, 167.14	Na_2SSO_3, Na_2SO_3	710.81	**Fe**$_2$O$_3$

from the corrosion products on the control coupon was due to sulfide. Although the specific binding energy for FeS is 161.6 eV, a tolerance of 0.3 eV might be related to energy loss features.[29] The two fitted S 2p peaks positions at 162.13 and 162.97 eV have been noted for $Na_2S_2O_3$, and the three peaks positions between 165.5 and 167.2 eV have been noted for Na_2SO_3.[27] S compounds on the coupons exposed to MFs were mainly in the forms of the $Na_2S_2O_3$ and Na_2SO_3, which are the intermediates of sulfate reduction.

According to Figure 7, the MFs gave rise to the formation of iron oxide instead of iron sulfide. The O 1s peak shifted to higher binding energy, and the O enrichment in the corrosion products increased at the higher MF in the form of FeO and Fe_2O_3. It is possible that a less dense biofilm and the presence of an MF increased the oxygen supply from the bulk fluid to the coupon surface. Oxygen molecules are paramagnetic. In an investigation of chemical corrosion, Costa et al.[11] observed that an MF increased oxygen transfer to the metal surface. Here, it can be concluded that the main corrosion products without an MF and with 2 and 4 mT MFs were FeS, FeO, and Fe_2O_3, respectively.

It is well-known that the main corrosion product in the presence of SRB is iron sulfide,[30] whereas the formation of corrosion products such as iron oxides is an abiotic process of chemical reactions in the presence of oxygen.[31] Combined with the SRB growth curve results, it is reasonable to conclude that the MFs inhibited SRB growth and changed the corrosion products, leading to the inhibition of the SRB corrosion of SS304.

4. CONCLUSIONS

The data from the 14-day experiments presented in this work showed that MFs reduced the population of planktonic SRB by almost 4 orders of magnitude and delayed the formation of SRB biofilms on SS304 coupons by at least two days. The coupon mass loss data indicated that the application of an MF considerably inhibited the SRB corrosion of SS304 and that a higher MF intensity led to less corrosion mass loss. The MF also significantly reduced both the number of pits caused by the SRB and the sizes of representative pits. EDX and XPS analyses of the corrosion products suggested that the main corrosion product was FeS without an MF, FeO with a 2 mT MF, and Fe_2O_3 with a 4 mT MF. These results show that the application of an MF could be an environmentally friendly method for mitigating MIC caused by SRB without biocides that could cause environmental problems and develop resistance from microbes.

AUTHOR INFORMATION

Corresponding Author

*E-mail: hongf_liu@163.com.

Author Contributions

[§]B.Z. and K.L. contributed equally to this work.

Notes

The authors declare no competing financial interest.

ACKNOWLEDGMENTS

This research was supported by the National Natural Science Foundation of China (No. 51171067) and the Natural Science Foundation of Shenzhen City (No. JC201005310696A). The authors acknowledge support from the Analytical and Testing Center of Huazhong University of Science and Technology.

REFERENCES

(1) Ručinskien, A.; Bikulčius, G.; Gudavičiūt, L.; Juzeliūnas, E. Magnetic field effect on stainless steel corrosion in $FeCl_3$ solution. *Electrochem. Commun.* **2002**, *4* (1), 86−91.

(2) Sueptitz, R.; Tschulik, K.; Uhlemann, M.; Schultz, L.; Gebert, A. Effect of high gradient magnetic fields on the anodic behaviour and localized corrosion of iron in sulphuric acid solutions. *Corros. Sci.* **2011**, *53* (10), 3222−3230.

(3) Sueptitz, R.; Tschulik, K.; Uhlemann, M.; Gebert, A.; Schultz, L. Impact of magnetic field gradients on the free corrosion of iron. *Electrochim. Acta* **2010**, *55* (18), 5200−5203.

(4) Guo, B.; Zhang, P.; Jin, Y.; Cheng, S. Effects of alternating magnetic field on the corrosion rate and corrosion products of copper. *Rare Metals* **2008**, *27* (3), 324−328.

(5) Yuan, B.; Wang, C.; Li, L.; Chen, S. Investigation of the effects of the magnetic field on the anodic dissolution of copper in NaCl solutions with holography. *Corros. Sci.* **2012**, *58*, 69−78.

(6) Lu, Z.; Huang, C.; Huang, D.; Yang, W. Effects of a magnetic field on the anodic dissolution, passivation and transpassivation behaviour of iron in weakly alkaline solutions with or without halides. *Corros. Sci.* **2006**, *48* (10), 3049−3077.

(7) Lu, Z.; Huang, D.; Yang, W. Probing into the effects of a magnetic field on the electrode processes of iron in sulphuric acid solutions with dichromate based on the fundamental electrochemistry kinetics. *Corros. Sci.* **2005**, *47* (6), 1471−1492.

(8) Lu, Z.; Yang, W. In situ monitoring the effects of a magnetic field on the open-circuit corrosion states of iron in acidic and neutral solutions. *Corros. Sci.* **2008**, *50* (2), 510−522.

(9) Lu, Z.; Huang, D.; Yang, W.; Congleton, J. Effects of an applied magnetic field on the dissolution and passivation of iron in sulphuric acid. *Corros. Sci.* **2003**, *45* (10), 2233−2249.

(10) Sueptitz, R.; Tschulik, K.; Uhlemann, M.; Schultz, L.; Gebert, A. Magnetic field effects on the active dissolution of iron. *Electrochim. Acta* **2011**, *56* (17), 5866−5871.

(11) Costa, I.; Oliveira, M. C. L.; de Melo, H. G.; Faria, R. N. The effect of the magnetic field on the corrosion behavior of Nd−Fe−B permanent magnets. *J. Magn. Magn. Mater.* **2004**, *278* (3), 348−358.

(12) Ji, W.; Huang, H.; Deng, A.; Pan, C. Effects of static magnetic fields on *Escherichia coli*. *Micron* **2009**, *40* (8), 894−898.

(13) Fojt, L.; Strašák, L.; Vetterl, V.; Šmarda, J. Comparison of the low-frequency magnetic field effects on bacteria *Escherichia coli*, *Leclercia adecarboxylata* and *Staphylococcus aureus*. *Bioelectrochemistry* **2004**, *63* (1−2), 337−341.

(14) Novák, J.; Strašák, L.; Fojt, L.; Slaninová, I.; Vetterl, V. Effects of low-frequency magnetic fields on the viability of yeast *Saccharomyces cerevisiae*. *Bioelectrochemistry* **2007**, *70* (1), 115−121.

(15) Filipič, J.; Kraigher, B.; Tepuš, B.; Kokol, V.; Mandic-Mulec, I. Effects of low-density static magnetic fields on the growth and activities of wastewater bacteria *Escherichia coli* and *Pseudomonas putida*. *Bioresour. Technol.* **2012**, *120* (0), 225−232.

(16) Kroupová, J.; Bártová, E.; Fojt, L.; Strašák, L.; Kozubek, S.; Vetterl, V. Low-frequency magnetic field effect on cytoskeleton and chromatin. *Bioelectrochemistry* **2007**, *70* (1), 96−100.

(17) Santos, L. O.; Alegre, R. M.; Garcia-Diego, C.; Cuellar, J. Effects of magnetic fields on biomass and glutathione production by the yeast *Saccharomyces cerevisiae*. *Process Biochem.* **2010**, *45* (8), 1362−1367.

(18) Kuang, F.; Wang, J.; Yan, L.; Zhang, D. Effects of sulfate-reducing bacteria on the corrosion behavior of carbon steel. *Electrochim. Acta* **2007**, *52* (20), 6084−6088.

(19) Dong, Z. H.; Shi, W.; Ruan, H. M.; Zhang, G. A. Heterogeneous corrosion of mild steel under SRB-biofilm characterised by electrochemical mapping technique. *Corros. Sci.* **2011**, *53* (9), 2978−2987.
(20) Zheng, B.; Zhao, Y.; Xue, W.; Liu, H. Microbial influenced corrosion behavior of micro-arc oxidation coating on AA2024. *Surf. Coat. Technol.* **2012**, *216* (15), 100−105.
(21) Videla, H. A.; Herrera, L. K. Microbiologically influenced corrosion: looking to the future. *Int. Microbiol.* **2005**, *8* (3), 169.
(22) Wen, J.; Zhao, K.; Gu, T.; Raad, I. I. A green biocide enhancer for the treatment of sulfate-reducing bacteria (SRB) biofilms on carbon steel surfaces using glutaraldehyde. *Int. Biodeterior. Biodegrad.* **2009**, *63* (8), 1102−1106.
(23) Yuan, S. J.; Pehkonen, S. O. Microbiologically influenced corrosion of 304 stainless steel by aerobic *Pseudomonas* NCIMB 2021 bacteria: AFM and XPS study. *Colloids Surf. B* **2007**, *59* (1), 87−99.
(24) Yuan, S.; Pehkonen, S.; Ting, Y.; Kang, E.; Neoh, K. Corrosion behavior of type 304 stainless steel in a simulated seawater-based medium in the presence and absence of aerobic *Pseudomonas* NCIMB 2021 bacteria. *Ind. Eng. Chem. Res.* **2008**, *47* (9), 3008−3020.
(25) Dong, Z. H.; Liu, T.; Liu, H. F. Influence of EPS isolated from thermophilic sulphate-reducing bacteria on carbon steel corrosion. *Biofouling* **2011**, *27* (5), 487−95.
(26) Videla, H. A. *Manual of Bicorrosion*; CRC Press: Boca Raton, FL, 1996; pp 121−135.
(27) Nguyen, T. M. P.; Sheng, X.; Ting, Y.-P.; Pehkonen, S. O. Biocorrosion of AISI 304 stainless steel by *Desulfovibrio desulfuricans* in seawater. *Ind. Eng. Chem. Res.* **2008**, *47* (14), 4703−4711.
(28) Moulder, J. F.; Chastain, J.; King, R. C. *Handbook of X-ray Photoelectron Spectroscopy: A Reference Book of Standard Spectra for Identification and Interpretation of XPS Data*; Physical Electronics: Eden Prairie, MN, 1995.
(29) Skinner, W. M.; Nesbitt, H. W.; Pratt, A. R. XPS identification of bulk hole defects and itinerant Fe 3d electrons in natural troilite (FeS). *Geochim. Cosmochim. Acta* **2004**, *68* (10), 2259−2263.
(30) Sun, C.; Xu, J.; Wang, F. Interaction of sulfate-reducing bacteria and carbon steel Q 235 in biofilm. *Ind. Eng. Chem. Res.* **2011**, *50* (22), 12797−12806.
(31) Duan, J.; Wu, S.; Zhang, X.; Huang, G.; Du, M.; Hou, B. Corrosion of carbon steel influenced by anaerobic biofilm in natural seawater. *Electrochim. Acta* **2008**, *54* (1), 22−28.

■ NOTE ADDED AFTER ASAP PUBLICATION

This paper posted ASAP December 19, 2013. A spelling error was corrected in the name of author Hongfang Liu, and this paper was reposted December 23, 2013.